Photoreactions with tensor-polarized deuterium target at VEPP–3

I.A.Rachek

Budker Institute of Nuclear Physics, Novosibirsk, Russia

September 18, 2009

- experimental approach
- two-body deuteron photodisintegration
- coherent pion photoproduction on the deuteron
- upgrade: almost-real photon tagging system
  - *charge pion photoproduction → next talk*

Method of Superthin Internal Target

- conception – in BINP
- first use – in BINP: VEP–1, VEPP–2, VEPP–3
- later – in many Laboratories:
  - electron storage rings: NIKHEF, Bates, HERA ...
  - ion rings: IUCF, CELCIUS, COSY ...
- allows to increase substantially the efficiency of utilization of target material and beam particles, thus making feasible measurements:
  - with exotic targets: polarized ones; of rare-isotopes, *etc.*
  - with exotic beams: positrons, antiprotons, ions of isotopes *etc.*
  - with slow or heavy or strong-ionizing reaction products.

review of the method:

S.G. Popov, Internal targets in storage rings of charged particles, Yad.Fiz. 62(1999)291

Atomic Beam Source

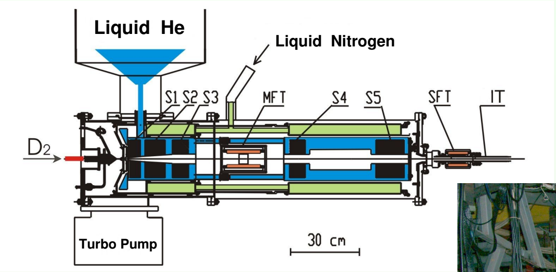

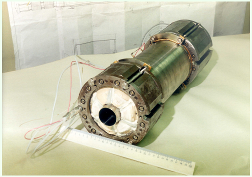

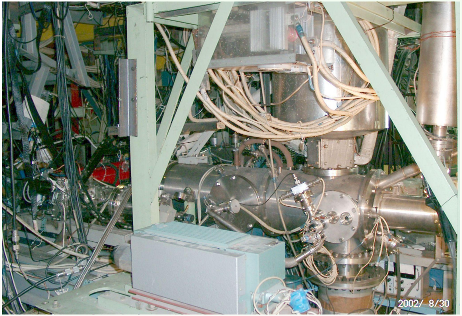

S1–S5 – sextupole magnets
MFT, SFT – RF-transition units
IT – inlet tube

Flux of deuterium atoms	$8 \cdot 10^{16}$ at/sec
Degree of tensor polarization	$> 98\%$
Degree of vector polarization	$< 2\%$

Storage Cell

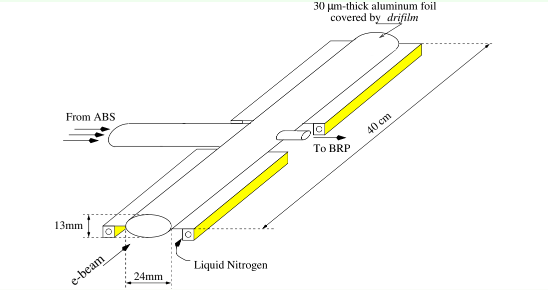

Gain over a jet target:

$$K = 1.1\frac{(L/2)^2}{D^2}\sqrt{\frac{T_{jet}}{T_{cell}}}$$

for our cell $K \approx 65$

New problems:

- depolarization in atom-wall collisions
- depolarization by mag. field of e-beam
- aperture limitation

Solutions:

- special wall coating – *drifilm*
- *mag. field strength* $>> H_c = 117\ Gs$
- *local modification of VEPP–3 beam optics*

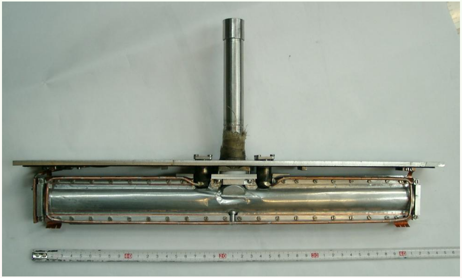

VEPP–3

VEPP–3 parameters

Electron energy	E_0	2 GeV
Mean beam current	I_0	150 mA
Energy spread	$\Delta E/E$	0.05%
RF HV magnitude	U_{72}	0.8 MV
revolution period	T	248.14 ns
bunch length	σ_L	15 cm
vertical beam size*	σ_z	0.5 mm
horizontal beam size*	σ_x	2.0 mm
vert. β-function*	β_z	2 m
horiz. β-function*	β_x	6 m
Injection beam energy	E_{inj}	350 MeV
Injection rate	$\dot{I}_{inj}$	$1.5{\cdot}10^9$ s^{-1}

* *parameters in the center of 2nd straight section*

shift graph (beam current vs. time)

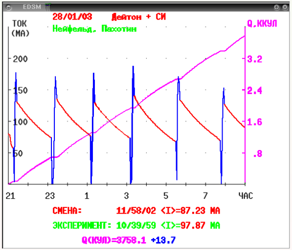

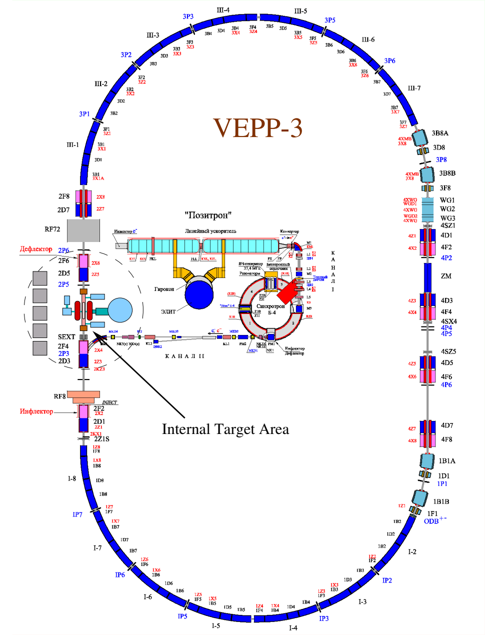

two-body deuteron photodisintegration

Heavy hydrogen was chosen as the element first to be examined, because **the diplon** *is the simplest of all nuclear systems and its properties are as important in nuclear theory as the hydrogen is in atomic theory.*
J. Chadwick and M. Goldhaber, Nature **134**(1934)237.

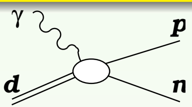

- two-body deuteron photodisintegration

$$\boxed{\gamma + d \longrightarrow p + n}$$

- T-matrix: $n = 2 \times 3 \times 2 \times 2 = 24 \xrightarrow{PC} 12$ complex amplitudes;
- in total $2n^2 = 288$ various observables, but only $2n - 1 = 23$ are independent
- any such "set-of-23" must include tensor asymmetries.

H. Arenhövel, W. Leidemann, E.L. Tomusiak, "Complete sets of polarization observables in electromagnetic deuteron breakup", FBS 28(2000)147.

Theoretical models

H.A.Bethe & R.Peierls, "Quantum theory of the diplon", Proc. Roy. Soc. A148(**1935**)146
. . . E1-multipole only, simplest NN-potential $V(r) = -V_0\ \delta(r)$:

$$\frac{d\sigma_{BP}}{d\Omega} = \frac{e^2}{\alpha^2}\frac{(\eta-1)^{3/2}}{\eta^3}\sin^2\theta, \qquad \sigma_{BP}(\omega) = \frac{8\pi}{3}\frac{e^2}{\alpha^2}\frac{(\eta-1)^{3/2}}{\eta^3}$$

where $\eta = E_\gamma/E_b$, $\alpha = \sqrt{M_d E_b}$, $E_b = 2.224\ MeV$

M.Schwamb and H. Arenhövel, Nucl. Phys. A690(2001)682
M. Schwamb, habilitation thesis, Johannes Gutenberg-Universität at Mainz, 2006

- coupled–channels approach: NN, $N\Delta$, πNN
- pion retardation in NN-potential and in MEC;
- mutual interactions between the involved three particles in the propagating πNN-system is taken into account nonperturbatively
- no free parameters with respect to deuteron photodisintegration, all parameters have been fitted in advance by considering other reactions.

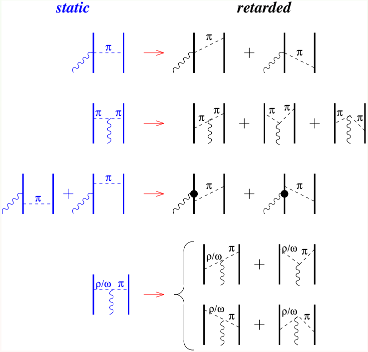

From static approach to meson retardation MEC.

Cross Section

in case of polarized spin-1 target and unpolarized photon beam:

$$\frac{d\sigma}{d\Omega} = \frac{d\sigma_0}{d\Omega}\Bigg\{1 - \sqrt{\frac{3}{4}}\,\mathbf{P_Z}\sin\theta_H\sin\phi_H \cdot \mathbf{T}_{11}(E\gamma,\theta_p^{CM})$$
$$+\sqrt{\frac{1}{2}}\,\mathbf{P_{ZZ}}\Bigg[\frac{3\cos^2\theta_H-1}{2}\cdot\mathbf{T}_{20}(E\gamma,\theta_p^{CM})$$
$$-\sqrt{\frac{3}{8}}\sin 2\theta_H\,\cos\phi_H\cdot\mathbf{T}_{21}(E\gamma,\theta_p^{CM})$$
$$+\sqrt{\frac{3}{8}}\sin^2\theta_H\,\cos 2\phi_H\cdot\mathbf{T}_{22}(E\gamma,\theta_p^{CM})\Bigg]\Bigg\}$$

$P_z = n_+ - n_-$ – *degree of target vector polarization*
$P_{zz} = 1 - 3\cdot n_0$ – *degree of target tensor polarization*
n_+, n_-, n_0 – *population numbers for spin projections* $+1$, -1 *and* 0, *respectively.*

Surface of constant density $\rho = 0.24 fm^{-3}$ *in deuteron*

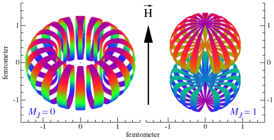

$P_{ZZ} = -2$ $P_{ZZ} = +1$

Almost–real photon approach

Electro-disintegration

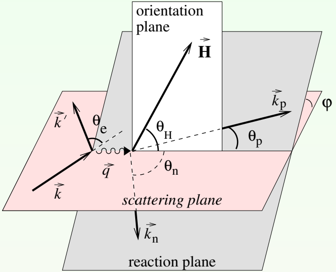

$$\theta_e \longrightarrow 0$$
$$Q^2 \longrightarrow 0$$

Photo-disintegration

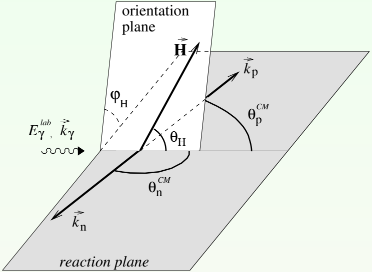

$$\textit{for } \theta_e \approx 0 : \qquad T_{2M}^{electro} \approx T_{2M}^{photo} \cdot \left(1 - \frac{\rho_L}{\rho_T}\right)$$

$$\rho_T = \frac{1}{2}\xi + \eta; \quad \rho_L = \xi^2; \quad \xi = \frac{Q^2}{|\vec{q}|^2}; \quad \eta = \tan^2\frac{\theta_e}{2}$$

$$\text{for small } \theta_e : \quad \rho_L/\rho_T = \left[\frac{1-r}{r(1-r/2)} \cdot \theta_e\right]^2, \quad \text{where } r = E_\gamma/E_e.$$

e.g. for $\theta_e^{cut} = 1^\circ$ and $E_\gamma/E_e = 0.1$ $\quad \delta \mathbf{T_{2M}}/\mathbf{T_{2M}} \leq \mathbf{10^{-3}}$

Detector Layout

- 2 pairs of arms in vertical plane:

arm	I	II
θ_p	20°-40°	55°-95°
θ_n	127°-145°	68°-92°
Δ_ϕ	25°	19°

- proton arm:
drift chambers + 3 scintillator layers

- neutron arm:
thin veto-counter + thick scintillator

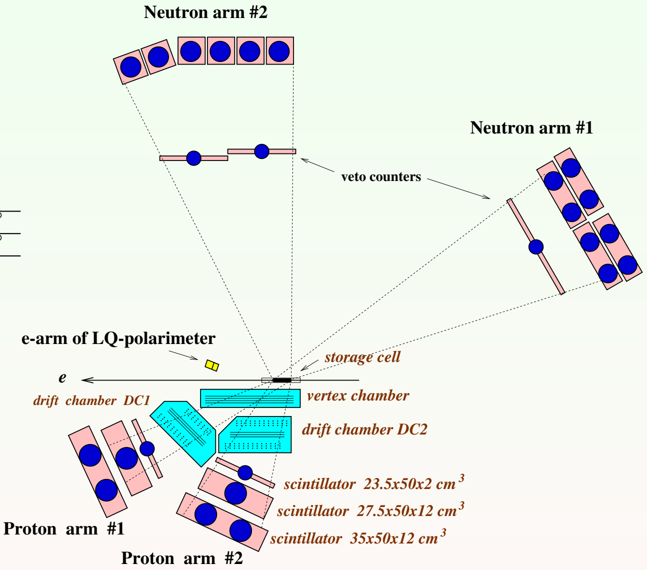

neutron arms

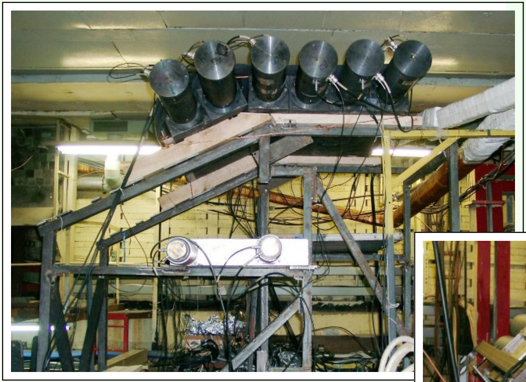

Separation of T_{IM}

Tensor asymmetry:

$$a^T = \sqrt{2}\,\frac{\sigma^+ - \sigma^-}{P_{zz}^+\sigma^- - P_{zz}^-\sigma^+} \to c_0\,T_{20} + c_1\,T_{21} + c_2\,T_{22}$$

$c_0\,(\theta_H, \phi_H)$, $c_1\,(\theta_H, \phi_H)$, $c_2\,(\theta_H, \phi_H)$

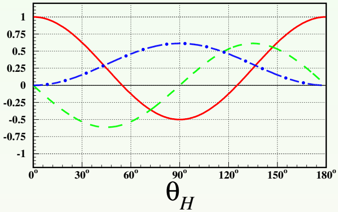

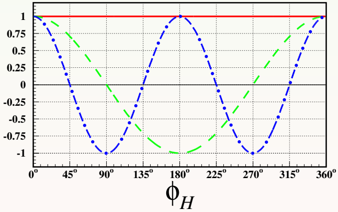

VEPP–3 (2003)		
$\phi_H = 180°$	$\theta_H = 180°$	$a_0 \sim c_0\,T_{20}$
	$\theta_H = 54.7°$	$a_1 \sim +c_1\,T_{21} + c_2\,T_{22}$
	$\theta_H = 125.3°$	$a_2 \sim -c_1\,T_{21} + c_2\,T_{22}$
		$\to \mathbf{T_{20} \sim a_0}$
		$\mathbf{T_{21} \sim a_1 - a_2}$
		$\mathbf{T_{22} \sim a_1 + a_2}$

regime 0

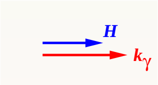

regime 1

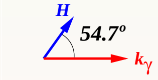

regime 2

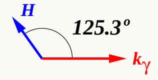

Data taking run

- 4-month run: Oct-2002 – Jan-2003
- electron energy 2000 MeV, mean beam current 80 mA, total beam integral 200 KCoulomb
- target thickness 3×10^{13} at/cm^2
- target polarization measured by the LQ-polarimeter: $P_{zz} = 0.341 \pm 0.025 \pm 0.013$
- raw events collected: 37.5M
  selected PD events: 540K

beam integral vs. time

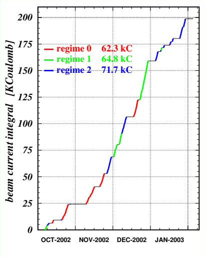

event distributions:

. . . vs. *photon energy*

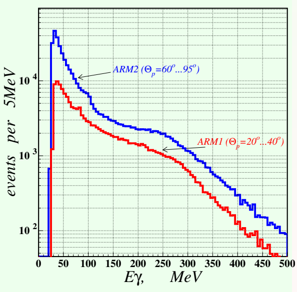

. . . vs. *proton angle*

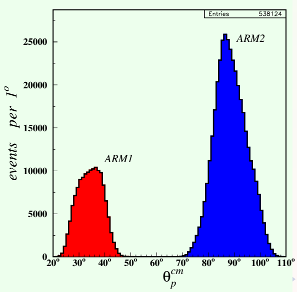

Results: as a function of E_γ

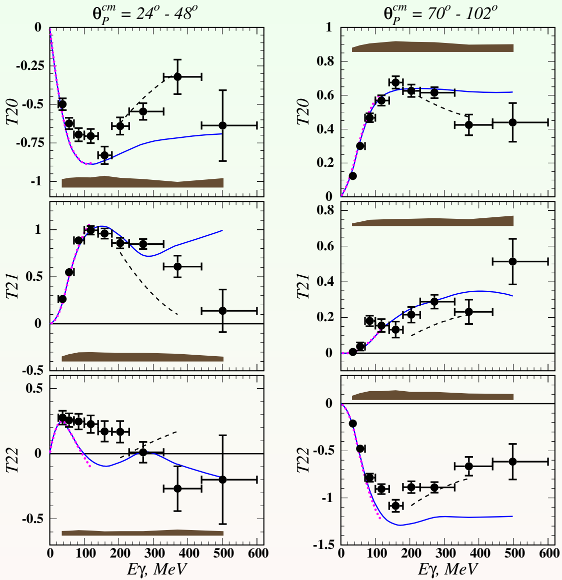

vertical bars – statistic errors

horizontal bars – bin sizes

shaded bands – systematic errors

Theoretical curves:

solid – K.-M.Schmitt&H.Arenhövel (1990), full calculation;

dotted – M.Levchuk (1995), full calculation;

dashed – M.Schwamb (2006).

I.A. Rachek *et al.*, Phys.Rev.Lett **98** (2007)182303

ingredients of the model: from M.Levchuk

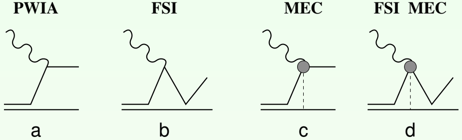

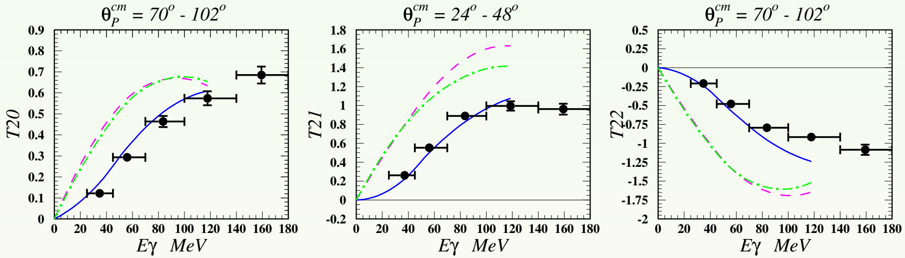

Plane Wave Impulse Approximation (a)

PWIA+ Final State Interaction (a+b)

PWIA+FSI+ Meson Exchange Currents (a+b+c+d)

Results: as a function of θ_p^{cm}, $E_\gamma = 25 \div 140$ MeV

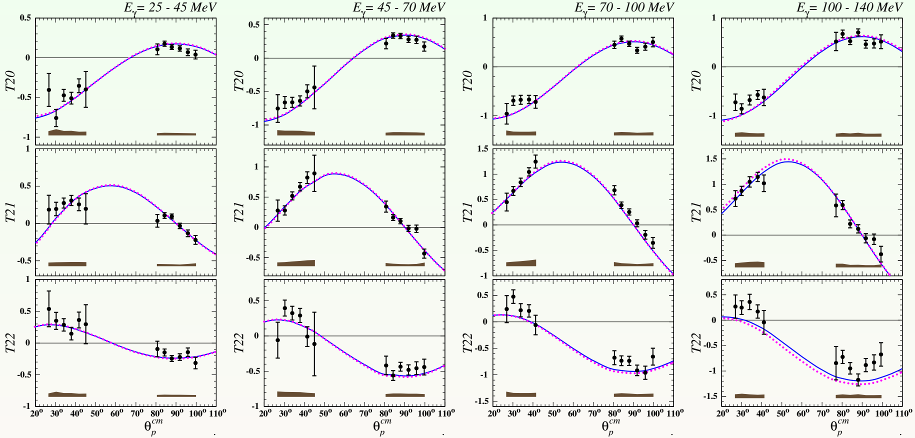

I.A. Rachek *et al.*, Phys.Rev.Lett **98** (2007)182303

Results: as a function of θ_p^{cm}, $E_\gamma = 140 \div 440$ MeV

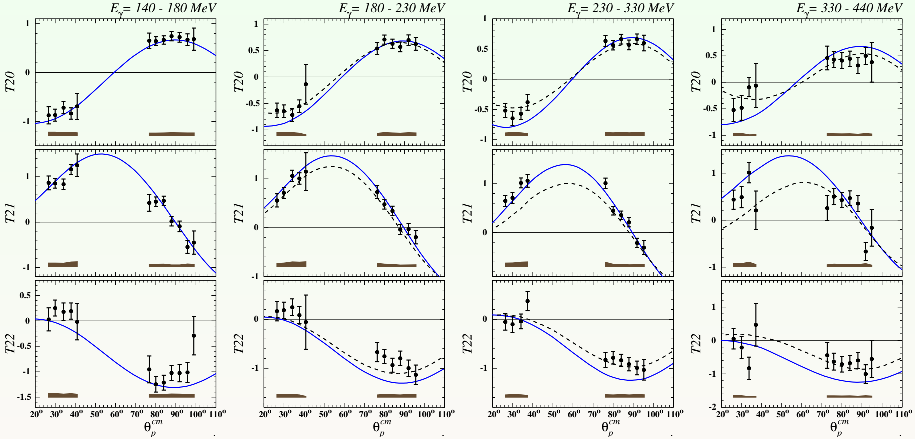

I.A. Rachek *et al.*, Phys.Rev.Lett **98** (2007)182303

Bonn (1989) tensor observable: Z–asymmetry

$$\mathbf{Z} = \sqrt{2}\mathbf{T}_{20} + \sqrt{3}\mathbf{T}_{22}$$

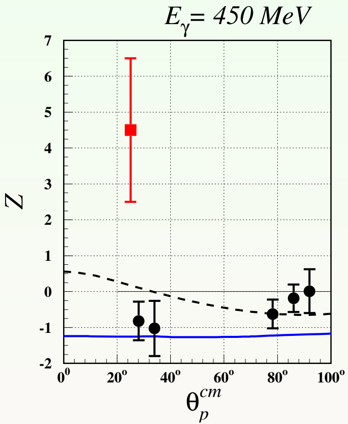

data: ■ Bonn [Z. Phys. C43, 375 (1989)]; ● Novosibirsk [2007]
curves: M.Schwamb&H.Arenhövel, K.-M.Schmitt&H.Arenhövel.

Summary

- New measurement of tensor analyzing powers T_{20}, T_{21} and T_{22} in deuteron photodisintegration, substantially enhancing the quality and kinematic span of the existing experimental data, has been performed.
- Accuracy of our data allow an accurate test of available models in a energy range $E_\gamma \lesssim 400$ MeV;
- Theoretical calculations provide excellent description of these polarization data below pion production threshold;
- Meson Exchange Currents play crucial role starting already at small photon energy;
- Above pion production threshold a very good description of T_{20} and T_{22} is demonstrated by a novel approach incorporating a π-MEC retardation mechanism
- the shape of angular dependencies of T_{IM} is described well and here better agreement is observed for Schwamb model as well;
- The remaining discrepancies could reflect the theoretical uncertainties or some missing or poorly modeled underlying dynamics, so *further improvement in theoretical models would be desirable.*

Coherent Neutral Pion Photoproduction on Deuteron

$$\gamma + d \to \pi^0 + d$$

the only pion photoproduction reaction on deuteron with two-body final state.

issues addressed:

- deuteron structure
- π^0 – deuteron elastic scattering
- pion photoproduction off neutron
- at threshold – chiral dynamics on neutron
- ...

P.Wilhelm and H.Arenhövel, Nucl. Phys. **A609**(1996)469 – couple-channel approach: *NN*, *N*π, *N*Δ

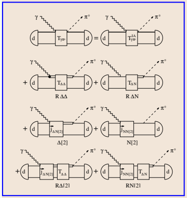

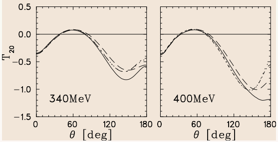

S.S.Kamalov, L.Tiator and C.Bennhold, Phys.Rev. **C55**(1997)98 *with FSI treated in the KMT multiple scattering approach*

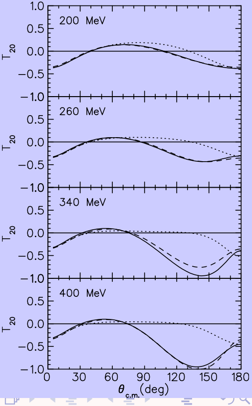

Detector Layout for coherent π^0 photoproduction

$\gamma + d \rightarrow \pi^0 + d'$ events have been selected from the statistics collected during the deuteron photodisintegration experiment.

- Data of one pair of arms used
- proton arm #1 detects deuteron
- neutron arm #1 detects one of γ-quantum from pion decay.

θ_d	$20^\circ \div 40^\circ$
Δ_ϕ	25°
E_d	$20 \div 70$ MeV

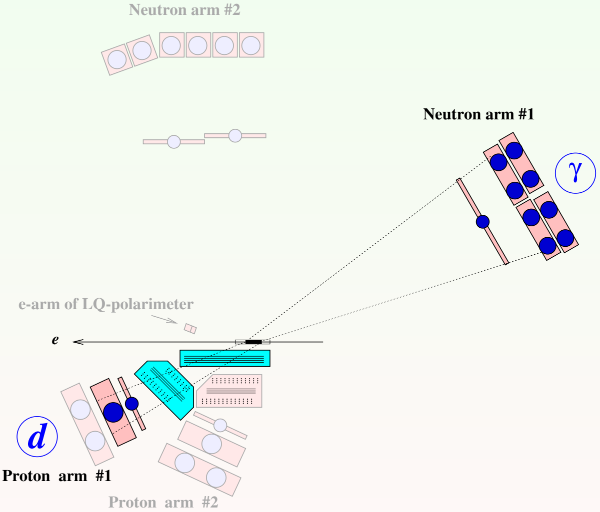

Background processes

Processes that may give $(d\gamma)$ coincidence in the detector:

- $\gamma d \rightarrow d'\pi^0\pi^0$
- $\gamma d \rightarrow d'\eta$
- $\gamma d \rightarrow d'\pi^0\pi^+\pi^-$

taking into account available cross section data as well as theoretical predictions one can conclude that process   process $\gamma d \rightarrow d'\pi^0$ dominates
and contribution of background processes does not exceed 2%

comparison of our data and GEANT4 simulation based on TAPS cross section data

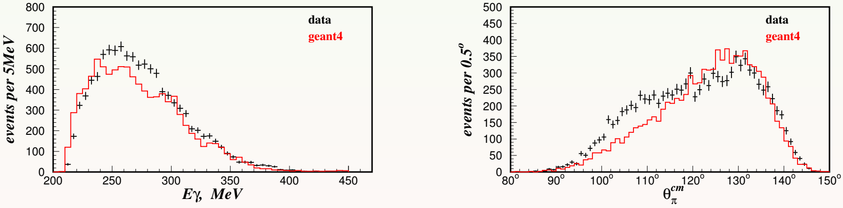

Results on coherent π^0 photoproduction

vs. E_γ *vs.* θ_π^{cm}

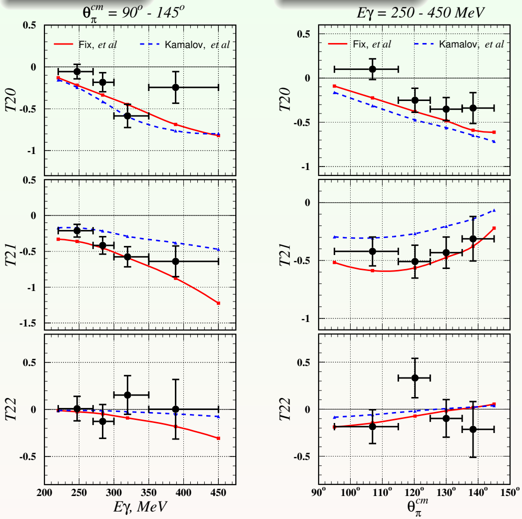

Vertical bars – statistical errors,
Horizontal bars – bin sizes;
Systematic error $\approx$ 9.4%

Theoretical curves:

solid – A.Fix, private communication,
dashed – S.S.Kamalov, L.Tiator and C.Bennhold, Phys. Rev. **C 55**(1997)98

D.M.Nikolenko, L.M. Barkov *et al.*, JETP Lett. **89**, 518 (2009)

Proposed experiment

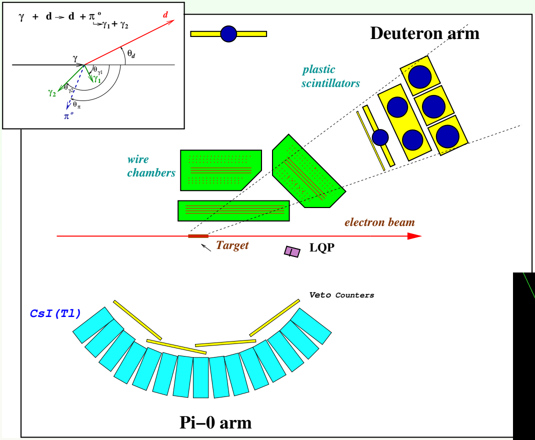

$E_\gamma = 250 \div 450$ MeV
$E_d = 25 \div 120$ MeV
$\theta_d = 18^\circ \div 35^\circ$
$\theta^{CM}_{\pi^0} = 100^\circ \div 140^\circ$
$\Delta\phi_d, \Delta\phi_{\pi^\circ} \approx 60^\circ$

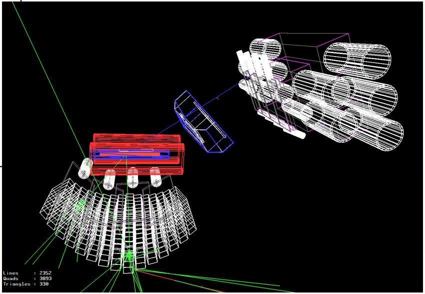

segmented calorimeter of 152 CsI(Tl) crystals $6 \times 6 \times 15 cm^3$ to measure both γ-quanta
$\rightarrow$ full kinematic reconstruction

Expected accuracy

Statistical accuracy for 100 kCoulomb beam integral (≈ 2 month run at VEPP–3)

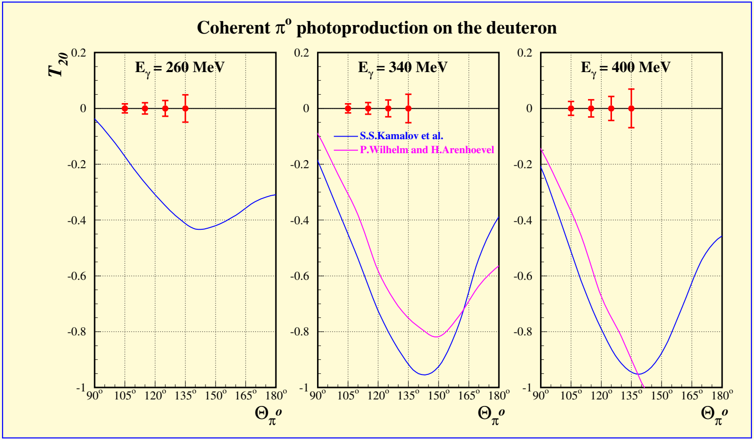

Almost–real photon tagger

Introduction of almost–real photon tagging system would allow

- a complete kinematic reconstruction, thus permitting a reliable rejection of the background processes
- to extend the measurements to higher photon energy;
- to determine the linear polarization of photon, thus enabling Σ–asymmetry measurements and double–polarization experiments

linear polarization of almost–real photon vs. its energy

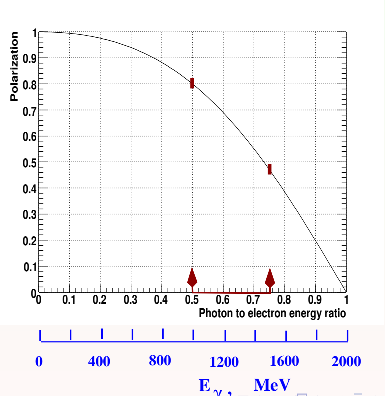

Layout of the Tagging System at the experimental section

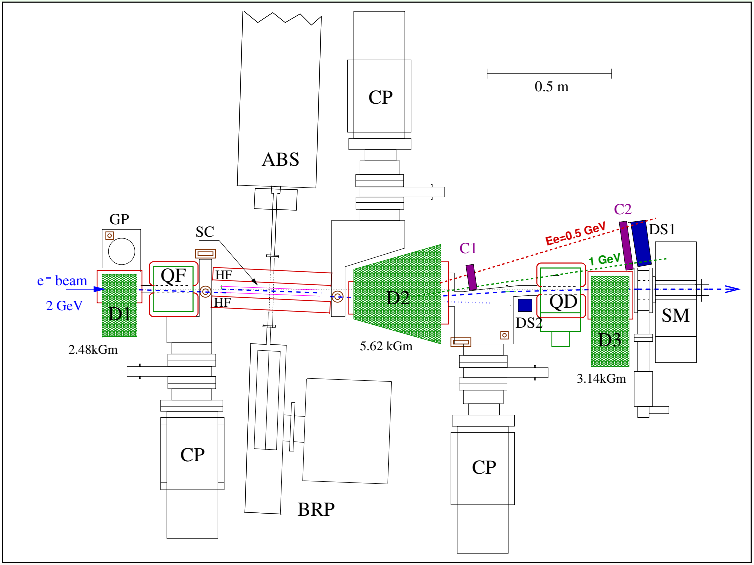

Top view at the experimental section of VEPP–3 with the chicane and the scattered electron tracker installed.

Tagger: expected energy and angular resolutions

$E_\gamma = (0.50 \div 0.75)E_e$

$\frac{\delta E_\gamma}{E_\gamma} = 1.4\% \ldots 0.3\%$

$\alpha_{\text{horiz}} = -30 \div +30$ mr

$\delta\alpha_{\text{horiz}} = 2$ mr

$\alpha_{\text{vert}} = -10 \div +10$ mr

$\delta\alpha_{\text{vert}} = 1$ mr

contributions to resolution at $E_e = 2$GeV

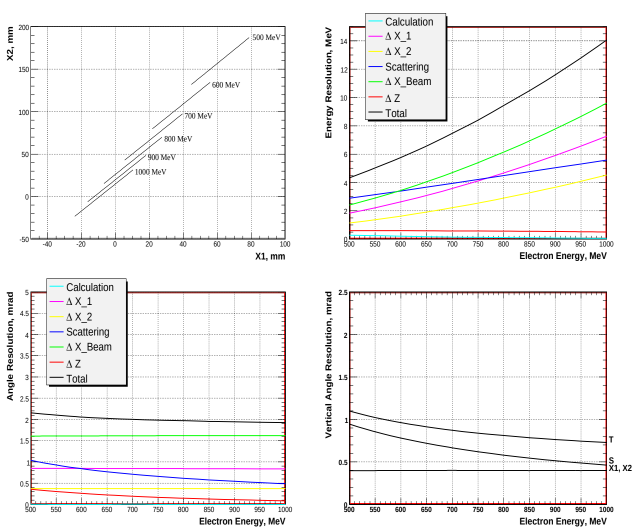

Example of experiment: deuteron photodisintegration at $E_\gamma = 1.0 \div 1.5$ GeV

transition from meson-baryon to quark-gluon picture of deuteron ?

- pQCD: Constituent Counting Rule, Hadron Helicity Conservation:
  $d\sigma/ds \rightarrow s^{-11}$ $p_y, c'_x, c'_z \rightarrow 0$ $\Sigma \rightarrow -1$ $T_{20} \rightarrow -\sqrt{2}$, $T_{21}, T_{22} \rightarrow 0$
- experimental results for photodisintegration at $\theta_p^{cm} = 90^\circ$:
  - cross section shows pQCD scaling above $E_\gamma \approx 1$ GeV
  - induced proton polarization vanishes at $E_\gamma \approx 1$ GeV as HHC predicts
  - but Σ asymmetry heads away from HHC at $E_\gamma = 1 \div 1.5$ GeV

cross section $\rightarrow s^{-11}$

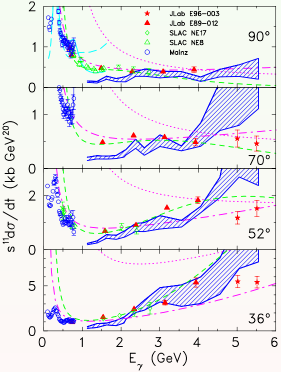

induced polarization $\rightarrow 0$

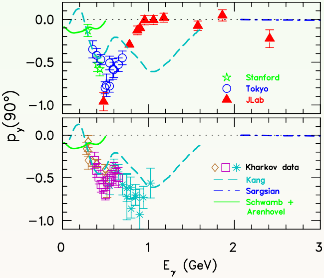

Σ asymmetry $\rightarrow -1$?

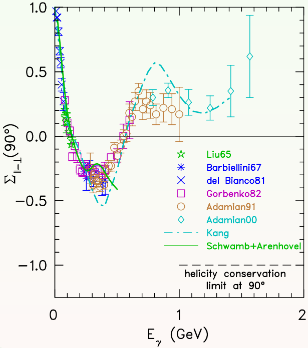

$T_{20} \rightarrow -\sqrt{2}$?, $T_{21}, T_{22} \rightarrow 0$?

Proposed detector layout

$E_\gamma = 1000 \div 1500$ MeV
$E_p = 500 \div 1000$ MeV
$E_n = 500 \div 1000$ MeV
$\theta_p = 45^\circ \div 85^\circ$
$\theta_p^{CM} = 70^\circ \div 110^\circ$
$\Delta\phi_p, \Delta\phi_n \approx 2 \times 60^\circ$

hadron sandwich

- 10 layers × (20mm Iron + 5+5mm Scintillator)
- 10 cm segmentation in both directions
- WLS fibers readout
  [G.I. Britvich *et al.*, NIM A564(2006)225]
- neutron detection efficiency: 60 . . . 70%
- angular resolution for neutrons 1.6°

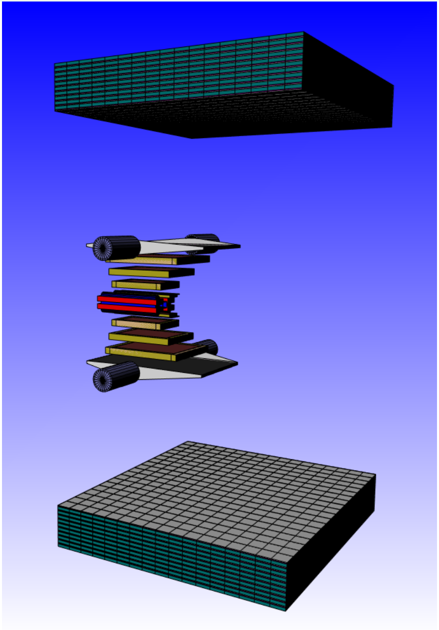

Expected accuracy

Expected accuracy for a 4 month run at VEPP-3

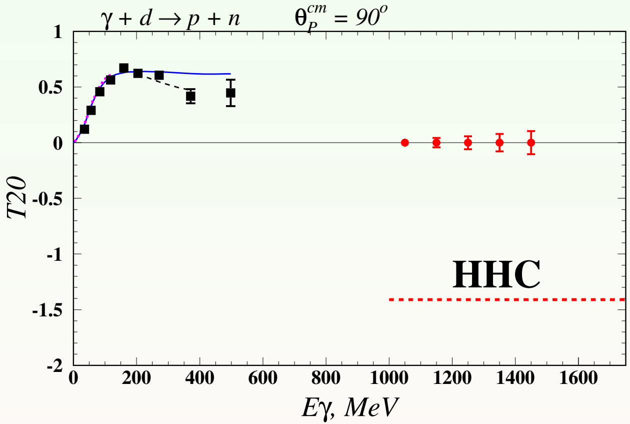

■ PRL 98 (2007) 182303; ● Proposed experiment

Participants

Novosibirsk Electron-Deuteron Collaboration

L.M. Barkov, V.F. Dmitriev, I.V. Karnakov, B.A. Lazarenko, S.I. Mishnev, D.M. Nikolenko, I.A. Rachek, R.Sh. Sadykov, Yu.V. Shestakov, D.K. Toporkov, L.I. Shekhtman and S.A. Zevakov
BINP, Novosibirsk, Russia

A.Yu. Loginov, A.N. Osipov, A.A. Sidorov and V.N. Stibunov
INR, Tomsk, Russia

R.J. Holt, D.H. Potterveld
ANL, Argonne, IL, USA

R. Gilman
Rutgers University, Piscataway, NJ, USA

H. de Vries
NIKHEF, Amsterdam, The Netherlands

S.L. Belostotsky, V.V. Nelyubin
INP, St.-Petersburg, Russia

H. Arenhövel
IKP, Johannes Gutenberg-Universität, Mainz, Germany